

Double Silyl Migration Converting $\text{ORe}[\text{N}(\text{SiMe}_2\text{CH}_2\text{PCy}_2)_2]$ to $\text{NRe}[\text{O}(\text{SiMe}_2\text{CH}_2\text{PCy}_2)_2]$ Substructures

Oleg V. Ozerov,[†] H el ene F. Gerard,[‡] Lori A. Watson,[†] John C. Huffman,[§] and Kenneth G. Caulton^{*†}

Department of Chemistry and Molecular Structure Center, Indiana University, Bloomington, Indiana 47405, and LSDSMS (UMR 5636), Universit e de Montpellier 2, 34095, Montpellier Cedex 5, France

Received June 25, 2002

The reaction of $(\text{R}_2\text{PCH}_2\text{SiMe}_2)_2\text{NM}$ ($\text{PNP}^{\text{R}}\text{M}$; $\text{R} = \text{Cy}$; $\text{M} = \text{Li}, \text{Na}, \text{MgHal}, \text{Ag}$) with L_2ReOX_3 [$\text{L}_2 = (\text{Ph}_3\text{P})_2$ or $(\text{Ph}_3\text{PO})(\text{Me}_2\text{S})$; $\text{X} = \text{Cl}, \text{Br}$] gives $(\text{PNP}^{\text{Cy}})\text{ReOX}_2$ as two isomers, mer,trans and mer,cis. These compounds undergo a double Si migration from N to O at 90  C to form $(\text{POP}^{\text{Cy}})\text{ReNX}_2$ as a mixture of mer,trans and fac,cis isomers. Additional thermolysis effects migration of CH_3 from Si to Re, along with compensating migration of halide from Re to Si. DFT calculations on various structural isomers support the greater thermodynamic stability of the POP/ReN isomer vs PNP/ReO and highlight the influence of the template effect on the reactivities of these species.

Introduction

The design of ligands intended for use in “aggressive” environments (strongly oxidizing or reducing or acidic conditions, high temperature, or high flux of energetic photons) obviously has to anticipate and avoid bonds vulnerable to such conditions. This becomes increasingly challenging when a polydentate ligand is multifunctional or when co-ligands or solvent incorporate functionality that can react with the chelate. Finally, polydentate ligand synthesis is based on certain bonds being “easily” formed. These bonds often are the result of nucleophilic/electrophilic combination, and the resulting bonds are often polar (single bonds) or reactive (e.g., $\text{C}=\text{N}$ double bonds).

A very attractive class of ligands has been widely applied in transition metal chemistry where a multifunctional and monoanionic ligand is useful. This ligand class is formed from commercially available $\text{HN}(\text{SiMe}_2(\text{CH}_2\text{Cl}))_2$ and nucleophilic phosphides R_2P^- (Scheme 1).¹ These ligands permit the incorporation of variable steric and electronic factors, and they incorporate numerous useful NMR spectral probes. Here, we will abbreviate $\text{N}(\text{SiMe}_2\text{CH}_2\text{PR}_2)_2$ as PNP^{R} .

In this work, we report how certain bonds in these ligands can be reactive to publicize how both N–Si and the Si–C bonds can be cleaved under frequently encountered conditions.

Results

Ligand Synthesis. The ligand employed in this study was synthesized by using a modification of Fryzuk’s preparation¹ of analogous compounds to obtain an improved yield. In the original preparation, two-thirds of the R_2PLi salt acted as a nucleophile in the formation of two P–C bonds. The remaining one-third of the R_2PLi merely functioned as a base to deprotonate $[(\text{PNP}^{\text{R}})\text{H}]$ in situ and was ultimately lost as R_2PH during the workup. We found that repeating the initial sequence in situ on one-third of the initial scale can convert valuable R_2PH formed in the reaction mixture to additional chelate product (Scheme 1). To investigate ways of introducing the PNP^{Cy} ligand into the Re coordination sphere, we sought to explore various PNP^{Cy} starting materials (Scheme 2). $[(\text{PNP}^{\text{Cy}})\text{Li}]$ (**1a**) typically contained approximately one molecule of Et_2O after crystallization. Recrystallization in the presence of TMEDA afforded $[(\text{PNP}^{\text{Cy}})\text{Li}\cdot\text{TMEDA}]$ (**1b**). Other simple derivatives of (PNP^{Cy}) can be prepared in a straightforward manner. Cation exchange² between $[(\text{PNP}^{\text{Cy}})\text{Li}\cdot\text{Et}_2\text{O}]$ or $[(\text{PNP}^{\text{Cy}})\text{Li}\cdot\text{TMEDA}]$ and NaOCMe_2Et in benzene/

* To whom correspondence should be addressed. E-mail: caulton@indiana.edu.

[†] Department of Chemistry, Indiana University.

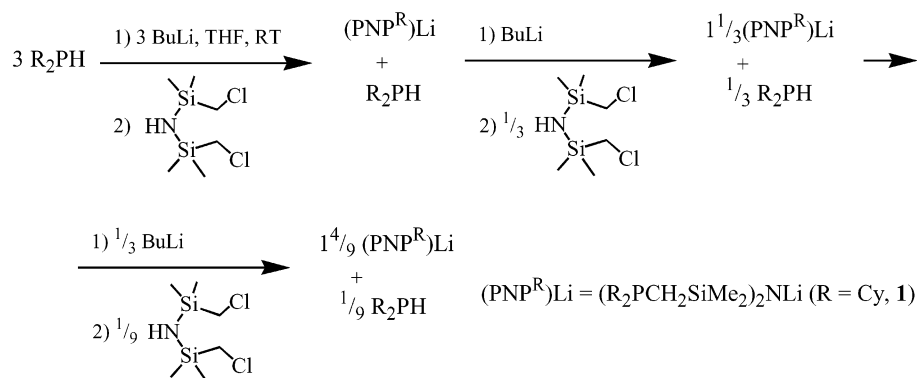
[§] Molecular Structure Center, Indiana University.

[‡] Universit e de Montpellier. Current address: Laboratoire de Chimie Theorique, Case, 137, Universite Pierre et Marie Curie, 4 Place Jussieu, 75252 Paris Cedex 6, France.

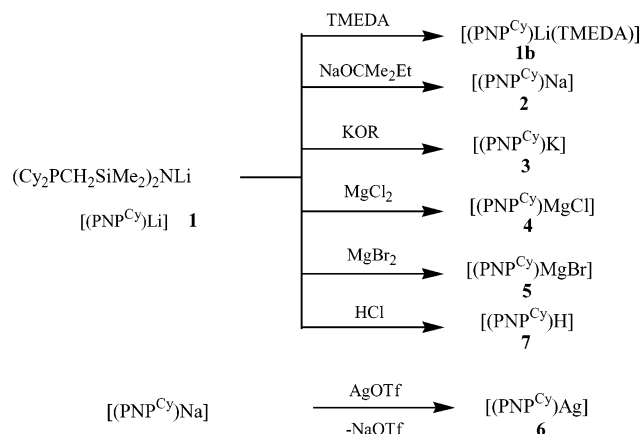
(1) (a) Fryzuk, M. D.; Carter, A.; Westerhaus, A. *Inorg. Chem.* **1985**, *24*, 642. (b) Coalter, J. N.; Watson, L. A.; Caulton, K. G. Unpublished results.

(2) (a) Lochmann, L.; Trekoval, J. *J. Organomet. Chem.* **1979**, *179*, 123. (b) Lochmann, L.; Trekoval, J. *Collect. Czech. Commun.* **1988**, *53*, 76. (c) Lochmann, L. *Eur. J. Inorg. Chem.* **2000**, 1115. (d) Ahlbrecht, H.; Schneider, G. *Tetrahedron* **1986**, *42*, 4729.

Scheme 1



Scheme 2



pentane mixtures afforded crystalline [(PNP^{Cy})Na] (**2**). Unlike the Li derivative, [(PNP^{Cy})Na] is very poorly soluble in pentane, benzene, and ether and is moderately soluble in THF. [(PNP^{Cy})K] (**3**) can be similarly prepared by cation exchange with KOR (R = mentoxide), but the apparently high solubility of [(PNP^{Cy})K] precluded its isolation. Reactions between [(PNP^{Cy})Li] or [(PNP^{Cy})Na] and anhydrous MgHal₂ provide [(PNP^{Cy})MgHal] (**4**, Hal = Cl; **5**, Hal = Br), which could be isolated as a solid or used in situ. We were unable to prepare [(PNP^{Cy})₂Mg], presumably because of the prohibiting steric bulk of the PNP^{Cy} ligand. [(PNP^{Cy})-Ag] (**6**) was prepared from [(PNP^{Cy})Na] and AgOTf in THF. [(PNP^{Cy})H] (**7**) was prepared by protonation of the Li or Na salt with 1 equiv of anhydrous HCl or Et₃NHCl and was used in situ.

Si–C and Si–N Bond Scission by Protolysis. It was found here that pincer ligands of the general formula HN-(SiMe₂CH₂PR₂)₂ [or its anionic form LiN(SiMe₂CH₂PR₂)₂], undergo Si–C cleavage, as well as cleavage of the Si–amide bond in the presence of excess alcohol. Four equivalents of alcohol can be consumed in the protolysis of **7** (Scheme 3). For example, reaction of **7** with phenol (ratio 1:5.3) in benzene is complete within 14 h at ambient temperature and 6 h at 60 °C (see Supporting Information), and forms Cy₂PMe and SiMe₂(OPh)₂ as confirmed by GC-MS and NMR analyses. The third product is assumed to be NH₃. Similar reactivities are observed with other PNP ligands: HN(SiMe₂-CH₂PBu^t)₂ is decomposed to ^tBu₂PMe and SiMe₂(OR')₂ upon treatment with excess alcohol.

This decomposition pathway of [(PNP^R)H] leading to the formation of R₂PMe was further confirmed by the formation of a known compound, [RuHCl(CO)(^tBu₂PMe)₂], isolated from the reaction of [(PNP^{t-Bu})Li] in MeOH (Scheme 3). The identity of [RuHCl(CO)(^tBu₂PMe)₂] was confirmed by comparison of ¹H, ³¹P, and ¹³C NMR data with the data for an authentic sample.³

Synthesis of Complexes. (a) From Re^{III}. Several commonly used Re starting materials were screened for their suitability for the introduction of the PNP^{Cy} ligand. Because of the lack of easily available Re^I complexes devoid of π-acid ligands such as CO, we focused our attention on higher Re oxidation states. Two Re^{III} complexes were chosen: [(PMe₂-Ph)₃ReCl₃]⁴ (**8**) and [(PPh₃)₂(MeCN)ReCl₃]⁵ (**9**). [(PMe₂-Ph)₃ReCl₃] (**8**) proved to be unreactive in salt metathesis attempts. It was inert toward **4**, **6**, and **7** even on prolonged exposure at high temperature. No reaction occurred between **8** and **1a** at ambient temperature in benzene or THF, whereas at higher temperature, [(PNP^{Cy})H] was produced along with unidentified byproducts (Scheme 4). The protonation of (PNP^{Cy}) anion in the reaction with **8** occurred more readily with **1b** and especially **2**. In the reactions of **1–7** with **9**, multiple products were formed in all cases. [(PNP^{Cy})H] was detected in the reactions of **1** or **2** with **9**.

(b) From Re^V. Re^V starting materials proved to be much more amenable to substitution by the PNP^{Cy} sources (Scheme 4). [(PPh₃)₂ReOHal₃]⁶ (**10**, Hal = Cl; **11**, Hal = Br) and [(PPh₃O)(Me₂S)ReOHal₃]⁷ (**12**, Hal = Cl; **13**, Hal = Br) reacted with anionic PNP^{Cy} compounds to yield corresponding [(PNP^{Cy})ReOHal₂] complexes (**14**, Hal = Cl; **15**, Hal = Br). The reaction mixtures from the reactions with **6** contained several soluble silver phosphine complexes, as was the case in reactions of **6** with **9**. The reaction of **7** with **10–13** produced mixtures of unidentified products. **1** and **4** (or **5**) performed the best and provided **14** (**15**) in excellent

(3) Gill, D. F.; Shaw, B. L. *Inorg. Chim. Acta* **1979**, 32, 19.

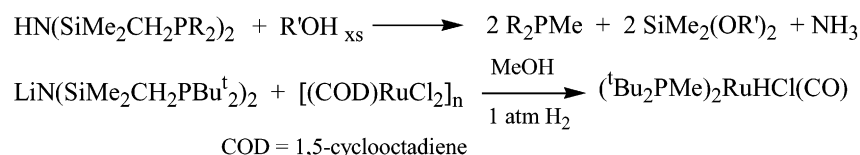
(4) (a) Parshall, G. W. *Inorg. Synth.* **1977**, 17, 111. (b) Douglas, P. G.; Shaw, B. L. *Inorg. Synth.* **1977**, 17, 64.

(5) Rouschias, G.; Wilkinson, G. *J. Chem. Soc. A* **1967**, 993.

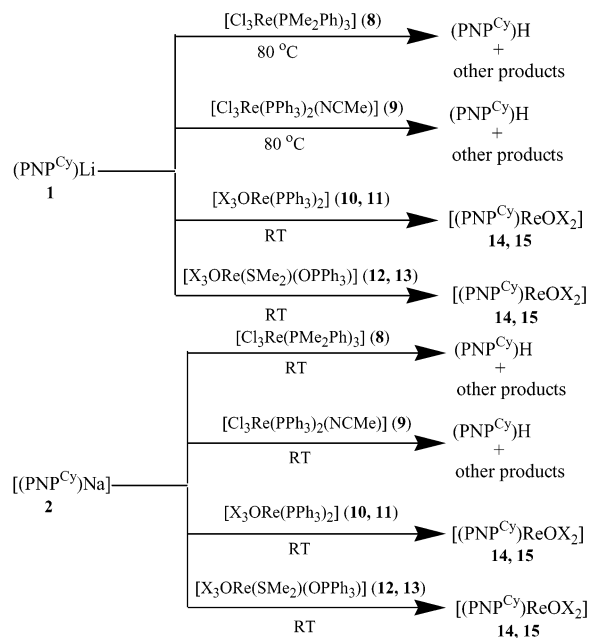
(6) (a) Johnson, N. P.; Lock, C. J. L.; Wilkinson, G. *J. Chem. Soc.* **1964**, 1054. (b) Johnson, N. P.; Lock, C. J. L.; Wilkinson, G. *Inorg. Synth.* **1967**, 9, 145. (c) Parshall, G. W. *Inorg. Synth.* **1977**, 17, 110.

(7) In the original preparation, the compounds were assigned as (PPh₃)(Me₂-SO)ReOX₃.^{8a} Later, it was shown that these compounds are, in fact, (Ph₃PO)(Me₂S)ReOX₃.^{8b} (a) Grove, D. E.; Wilkinson, G. *J. Chem. Soc. A* **1966**, 1224. (b) Bryan, J. C.; Stenkamp, R. E.; Tulip, T. H.; Mayer, J. M. *Inorg. Chem.* **1987**, 26, 2283.

Scheme 3



Scheme 4



yield as judged by NMR spectroscopy. **12** (**13**) is a more suitable precursor than **10** (**11**) because of the easier separation from byproducts.

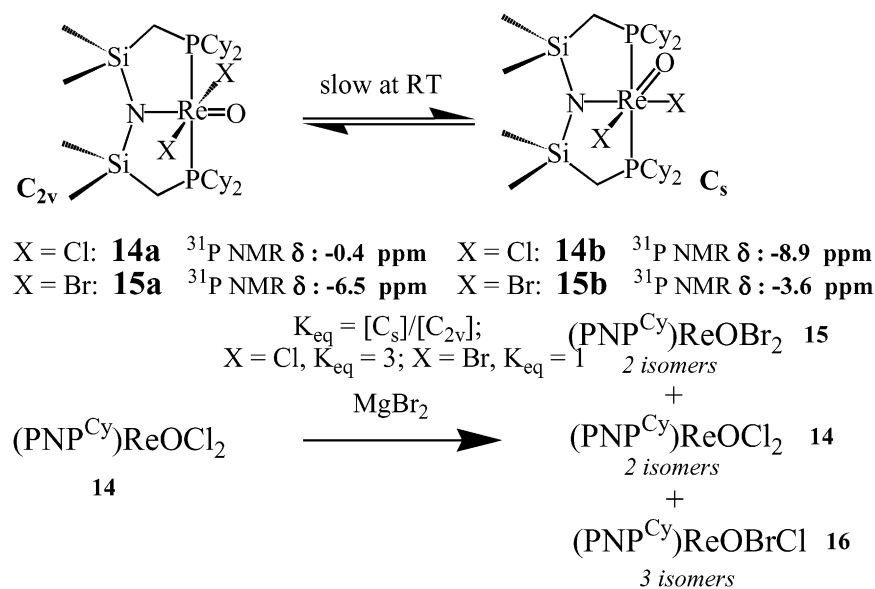
(c) **Stereoisomers.** Green complexes **14** and **15** were isolated as mixtures of *mer,trans* (**14a**, **15a**) and *mer,cis* (**14b**, **15b**) isomers (Scheme 5). The PNP^{Cy} ligand offers certain NMR spectroscopic probes to determine the symmetry of PNP complexes. In addition to the ^{31}P NMR signals, the number of signals from the Si–Me groups in the ^1H NMR

spectra, located in an otherwise desolate region, can be informative. Consistent with the *mer,trans* assignment, **14a** and **15a** each displays a single resonance in the ^{31}P NMR spectrum and a single Si–Me resonance in the ^1H NMR spectrum. Each **14b** and **15b** displays a single ^{31}P NMR resonance and two Si–Me resonances of equal intensity in the ^1H NMR spectrum. This is consistent with the *mer,cis* assignment; however, a *fac* geometry for the PNP^{Cy} ligand for **14b** and **15b** cannot be ruled out on the basis of these data alone. The following experiment was useful in elucidating this issue. Reaction of **14** with MgBr_2 in $\text{C}_6\text{D}_6/\text{Et}_2\text{O}$ ($\text{Re}/\text{Mg} = 1:1$) yields products of halide scrambling. Both isomers of each **14** and **15** are observed in the mixture by ^{31}P NMR spectroscopy, along with three other singlets that can be assigned to $[(\text{PNP}^{\text{Cy}})\text{ReOClBr}]$ (**16**). The fact that each of these three signals is a singlet is consistent with only the *mer* arrangement of the PNP^{Cy} ligand because any isomer of **16** with the *fac*- PNP^{Cy} arrangement should display in equivalent phosphines by ^{31}P NMR spectroscopy. The preference for the *mer*-PNP geometry is further supported by the computational results (*vide infra*).

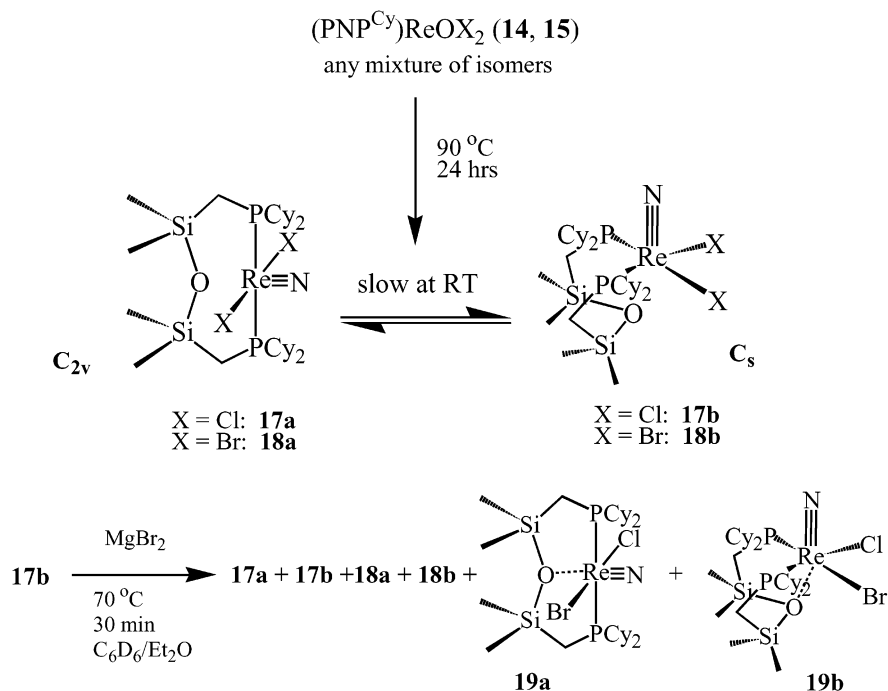
Thermolytic Si–N Bond Scission and Silyl Migration.

14 and **15** are thermally unstable and undergo a remarkable N/O transposition reaction at elevated temperatures (Scheme 6). Heating separate samples of **14** and **15** at 80 – 100°C in C_6D_6 for 24 h results in the formation of the new complexes **17** and **18**, respectively. Two isomers of each **17** and **18** are observed and the exact ratio depends on the handling history. The interconversion between the isomers at ambient temperature is slow in solution and does not occur in the solid

Scheme 5



Scheme 6



state. **17a** and **18a** each display a single resonance in the ³¹P NMR spectrum and a single Si–Me resonance in the ¹H NMR spectrum. This is consistent with the *mer,trans* geometry. **17b** and **18b** each display a single resonance in the ³¹P NMR spectrum and two Si–Me resonances of equal intensity in the ¹H NMR spectrum. This is consistent with both the *fac,cis* and the *mer,cis* geometries. A halide scrambling experiment (Scheme 6) produced two isomers of each **17**, **18**, and **19**. A singlet resonance in the ³¹P NMR spectrum corresponded to **19a** (*mer*-POP), but the other isomer of [(POP^{Cy})ReNBrCl], **19b**, displayed an AB pattern with a *J*_{PP} typical of *cis*-coordinated phosphines, supporting a *fac*-POP geometry. An X-ray diffraction study confirmed a *fac,cis* geometry for **17b** (Figure 1) and a *mer,trans* geometry for **18a** (Figure 2). The preference for the observed isomers is also supported by computational evidence (vide infra). The thermal transformation of **14** (**15**) into **17** (**18**) also occurs in the solid state, albeit more slowly. Thus, heating a sample of **14** for 5 days at 115 °C produced **17a** at 95% conversion with virtually no **17b** detected. However,

heating a sample of **14** for 2 days at 90 °C produced a mixture of **14a**, **14b**, **17a**, and **17b**. These results imply that not only the transformation of **14** into **17** but also the interconversion between the isomers of **14** and **17** is possible at elevated temperatures in the solid state.

Methyl/Halide Interchange. Even more remarkable is the fact that the nitrido complexes **17** and **18** are not the final thermodynamic products. NMR analysis of C₆D₆ solutions of **17** that were heated at 80–110 °C for several days revealed the formation of two new products (Scheme 7). These two compounds displayed AB patterns in their ³¹P NMR spectra with almost identical chemical shifts and *J*_{PP} coupling constants (**20a**: 24.7, 22.8 ppm, *J*_{PP} = 168 Hz. **20b**: 24.8, 22.7 ppm, *J*_{PP} = 166 Hz). From the fact that *each* of these new compounds shows *three* Si–Me signals of equal intensity, we conclude that one of the methyl groups on the Si atom is no longer present on the pincer ligand backbone in **20**. Indeed, ¹³C NMR analysis of the mixture revealed the presence of two resonances at –14.8 and –15.5 ppm, each appearing as a triplet due to coupling to the two P atoms (*J*_{CP} = 5.5 Hz).⁸ ¹³C DEPT experiments demon-

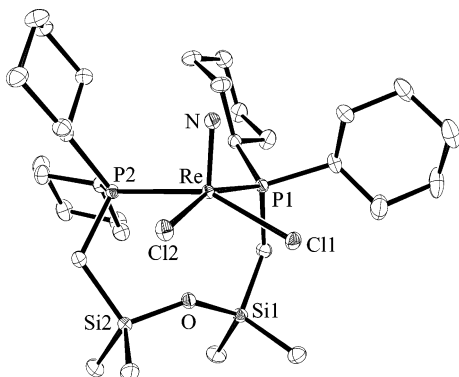


Figure 1. ORTEP²⁸ view of **17b** drawn with 50% probability ellipsoids. Hydrogen atoms are omitted for clarity.

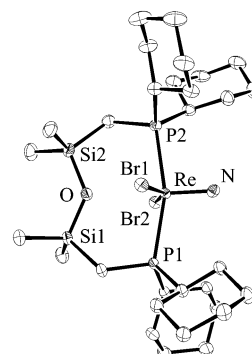
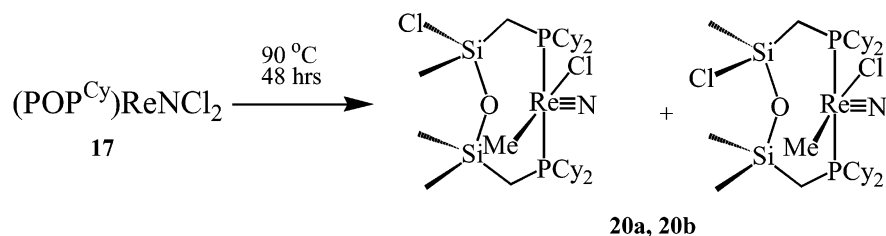


Figure 2. ORTEP²⁸ view of **18a** drawn with 50% probability ellipsoids. Hydrogen atoms are omitted for clarity.

Scheme 7



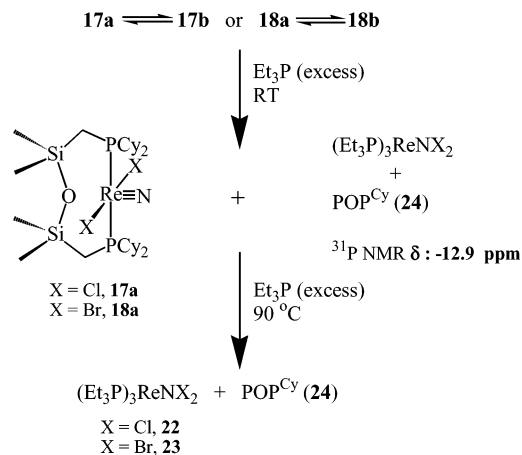
strated that each of these signals corresponds to a CH_3 group. The magnitude of the J_{PP} coupling constant rules out a cis arrangement of the phosphine arms. It is consistent with the transoid geometry similar to that observed in the structure of **18a**. We therefore assign these new products as **20a** and **20b**, the two possible diastereomers for the proposed structure: the Cl substituent on the Si atom is either syn or anti to Me on Re. We could not achieve more than 50% conversion to **20** even after 8 days of heating **17** at 90 °C, so we could not isolate **20** in a pure form. Heating **17** at higher (120 °C) temperatures in toluene- d_8 did not provide for a higher conversion, so it is likely that, at high temperatures, **17** and **20** exist in an equilibrium that is temperature-dependent. A similar thermal transformation occurs with the dibromo analogue **18**, but it requires longer reaction times and even after 7 days at 90 °C, the concentration of the proposed **21** was quite small.

Displacement of the POP^{Cy} Ligand by Et_3P . The reduction of Re^{V} oxo complexes by deoxygenation with trialkylphosphines is a common technique;^{5–7,9} however, complexes **14** and **15** show no reaction with Et_3P at ambient temperature. At 80 °C in the presence of 3 or more equivalents of Et_3P , **14** (**15**) is quantitatively (NMR) converted into **22** (**23**)¹⁰ and free POP^{Cy} (**24**) in several hours (Scheme 8). Thus, heating **14** (**15**) with a simple phosphine results in N-to-O silyl migration and displacement of a tridentate ligand! Control experiments showed that **17b** (**18b**) reacts with an excess of Et_3P at ambient temperature in the time of mixing to form **22** (**23**) and **24**, whereas **17a** (**18a**) requires longer reaction times and elevated temperature. Evidently, excess Et_3P displaces POP^{Cy} from **17** and **18** formed in situ from **14** or **15**. $[(\text{Et}_3\text{P})_3\text{ReNHal}_2]$ (**22**, **23**)¹⁰ and **24** were identified on the basis of NMR and mass-spectrometry data.

Discussion

Protolytic Decomposition. Many common preparative methods in the chemistry of later transition metals, and Re

Scheme 8

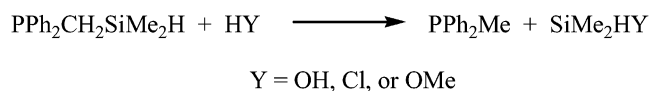


in particular, employ alcohols, water, and acids as solvents or reagents.¹¹ It is evident then that the resistance of the ancillary ligands to such conditions must be established. We found that alcohols and water easily disassemble the PNP ligand framework. The PNP^{Cy} moiety can be regarded as a derivative of the $(\text{Me}_3\text{Si})_2\text{N}$ parent in which two of the hydrogens are substituted by a Cy_2P group. The cleavage of the N–Si bonds is then to be expected because hexamethyldisilazane is a well-known silylation reagent.¹² The cleavage of the Si– CH_2PR_2 bond also has precedence. Facile silyl-group cleavage from a carbon atom attached to a phosphorus substituent has been reported for $\text{Ph}_2\text{PCH}_2\text{SiMe}_2\text{H}$ (Scheme 9).¹³ The overall protolytic decomposition of the PNP framework is rationalized in terms of the kinetic lability of these Si–N and Si–C bonds and the high thermodynamic affinity of Si to form Si–O bonds.

- (10) (a) Chatt, J.; Garforth, J. D.; Johnson, N. P.; Rowe, G. A. *J. Chem. Soc.* **1964**, 1012. (b) Chatt, J.; Falk, C. D.; Leigh, G. J.; Paske, R. J. *J. Chem. Soc. A* **1969**, 2288.
- (11) (a) Baudry, D.; Ephritikhine, M.; Felkin, H. *J. Organomet. Chem.* **1982**, 224, 363. (b) Kelle Zeiher, E. H.; DeWit, D. G.; Caulton, K. G. *J. Am. Chem. Soc.* **1984**, 106, 7006. (c) Jones, W. D.; Maguire, J. A. *Organometallics* **1987**, 6, 1301. (d) Carr, S. W.; Fowles, E. H.; Fontaine, X. L. R.; Shaw, B. L. *J. Chem. Soc., Dalton Trans.* **1990**, 573. (e) Smith, K. J.; Ondracek, A. L.; Gruhn, N. E.; Lichtenberger, D. L.; Fanwick, P. E.; Walton, R. A. *Inorg. Chim. Acta* **2000**, 300–302, 23. (f) Abel, E. W.; Bennett, M. A.; Wilkinson, G. *J. Chem. Soc.* **1959**, 3178. (g) Esteruelas, M. A.; Werner, H. *J. Organomet. Chem.* **1986**, 303, 221. (h) Gruenwald, C.; Gevert, O.; Wolf, J.; Gonzalez-Herrero, P.; Werner, H. *Organometallics* **1996**, 15, 1960.
- (12) (a) Cossy, J.; Pale, P. *Tetrahedron Lett.* **1987**, 28, 6039. (b) Firouzabadi, H.; Karimi, B. *Synth. Commun.* **1993**, 23, 1633. (c) Karimi, B.; Golshani, B. *J. Org. Chem.* **2000**, 65, 7228.
- (13) (a) Brost, R. D.; Bruce, G. C.; Grundy, S. L.; Stobart, S. R. *Inorg. Chem.* **1993**, 32, 5195. (b) Brost, R. D.; Bruce, G. C.; Stobart, S. R. *J. Chem. Soc., Chem. Commun.* **1986**, 21, 1580. (c) Eaborn, C.; Retta, N.; Smith, J. D. *J. Chem. Soc., Dalton Trans.* **1983**, 905.

- (8) Me groups in the following Re^{V} complexes were reported to resonate in the negative region of the ¹³C NMR spectrum: Cp*Re(O)MeX (X = Cl, alkyl);^{9a,b} *trans*-[(R₃P)₂Re(O)Me₂]⁺ BF₄[–].^{9c} (a) Herrmann, W. A.; Floeel, M.; Herdtweck, E. *J. Organomet. Chem.* **1988**, 358, 321. (b) Herrmann, W. A.; Felixberger, J. K.; Anwender, R.; Herdtweck, E.; Kiprof, P.; Riede, J. *Organometallics* **1990**, 9, 1434. (c) Hoffman, D. M.; Wierda, D. A. *Polyhedron* **1989**, 8, 959.
- (9) (a) Conry, R. R.; Mayer, J. M. *Inorg. Chem.* **1990**, 29, 4862. (b) Seymore, S. B.; Brown, S. N. *Inorg. Chem.* **2000**, 39, 325. (c) Chakraborty, I.; Bhattacharyya, S.; Banerjee, S.; Dirghangi, B. K.; Chakravorty, A. *J. Chem. Soc., Dalton Trans.* **1999**, 3747. (d) Bhattacharyya, S.; Chakraborty, I.; Dirghangi, B. K.; Chakravorty, A. *Inorg. Chem.* **2001**, 40, 286.

Scheme 9



Influence of the Cation on the Reactivity of PNP^{Cy} Salts. The difference in behavior of Li, Mg, Na, and Ag derivatives toward various Re starting materials can be justified by the following arguments. All of the donor atoms of the PNP^{Cy} ligand in [(PNP)Ag] are covalently bound to the silver atom, which makes it a poor PNP^{Cy} transfer reagent. In addition, the propensity of silver to form mixed-halide bridged phosphine complexes is well-documented,¹⁴ and it complicates the reactions where the transfer of the PNP^{Cy} ligand to Re does occur. In the series of **1**, **2**, **4**, and **5**, the difference in reactivity can be justified by the differences in the relative basicities and nucleophilicities of these compounds. Hexamethyldisilazide salts are known as poorly nucleophilic Brønsted bases because of the bulk of the anion;¹⁵ introduction of the voluminous Cy₂P groups only increases steric encumbrance. It is possible that the first step in the introduction of the PNP^{Cy} moiety into the Re coordination sphere occurs via coordination of one of the phosphine arms and not of the amido fragment. Indeed, **9–13** are known to react easily with neutral ligands such as phosphines by ligand displacement because of the lability of the uncharged ligands. Where such ligand displacement is kinetically retarded, such as in the case of **8**, secondary modes of reactivity can be explored by the PNP^{Cy} compound. Deprotonation of a coordinated phosphine is one alternative pathway, which is apparently operative in the reactions of **8** with **1** and **2** where we observed the formation of [(PNP^{Cy})H]. It might appear that the basicity of a disilylamido is insufficient to remove a proton from a weakly acidic coordinated PhPMe₂.¹⁶ Yet, most likely, the deprotonation is thermodynamically driven by the formation of LiCl or NaCl and not by the protonation of a stronger base, i.e., **1** or **2** assists in the E2 elimination process. It is also well-documented that sodium amides and alkyls act as stronger bases than their Li counterparts² and that TMEDA complexation increases the basicity of alkyllithiums.¹⁷ The Mg derivative can be expected to be an even milder, less basic reagent, and **4** simply does not react with **8** at all.

Thermolysis of Re Complexes. There is precedent for cleavage of N–Si bonds when amide N is coordinated to

Zr, Ta, or Mo.¹⁸ The rearrangement of **14** (**15**) into **17** (**18**) is thermodynamically favorable and irreversible, but it apparently has a high activation energy, as the transformation is slow even at elevated temperatures. The thermodynamic driving force behind the silyl migration is doubtless the formation of strong Si–O bonds. It is likely that the process occurs as a nucleophilic attack of the oxygen of the oxo group on the Si center. Presumably, this demands a cis geometry of the oxo and amido groups and an approximate syn orientation of the O and Si atoms. The high activation energy might be due to the deformation of the PNP framework required to bring the Si atom into the proximity of the oxo group. Perhaps, dissociation of a phosphine arm is necessary to accomplish this step. The favorable thermodynamics of the migration of a closely related silyl group in a PNP ligand from an amide nitrogen to an acyl oxygen have been reported;¹⁹ in that case, the reaction is even faster than those we report.

Solid-State Structures of 17b and 18a. An X-ray diffraction study (Figure 1) revealed that **17b** exhibits an approximate tetragonal pyramid geometry about the Re center, with the nitrido ligand occupying the apical position, if the Re–O interaction is not taken into account. The Re–O distance of 2.856(3) Å is quite long and can only be considered as incipient or weak bonding. However, the sum of the van der Waals radii of O (1.42 Å) and Re (using the literature²⁰ value for Pt, 1.75 Å) is 3.17 Å, which ensures that the 2.856(3) distance does involve some interaction. Disilyl ethers are weak O-donors, and the Re–O bond is further weakened by the strong trans influence of the nitrido ligand. The weak interaction that we believe exists between the Re and O atoms is undoubtedly made possible by the chelate effect. Computational results help address this issue (vide infra). The angles between the nitrido ligand and each of the basal ligands are greater than 90° as is typical for metal nitride structures.²¹ The angle between the *cis*-phosphines of 102.97(3)° is larger than the angle of 80.73–(3)° between *cis*-chlorides, presumably a consequence of the steric bulk of the phosphine groups. The Re–N bond distance of 1.651(3) Å is typical for rhenium nitrido complexes.²¹

- (14) (a) Sanghani, D. V.; Smith, P. J.; Allen, D. W.; Taylor, B. F. *Inorg. Chim. Acta* **1982**, *59*, 203. (b) Attar, S.; Alcock, N. W.; Bowmaker, G. A.; Frye, J. S.; Bearden, W. H.; Nelson, J. H. *Inorg. Chem.* **1991**, *30*, 4166. (c) Baker, L.-J.; Bowmaker, G. A.; Camp, D.; Effendy; Healy, P. C.; Schmidbaur, H.; Steigelmann, O.; White, A. H. *Inorg. Chem.* **1992**, *31*, 3656.
- (15) (a) Stork, G.; Uyeo, S.; Wakamatsu, T.; Grieco, P.; Labovitz, J. J. *Am. Chem. Soc.* **1971**, *93*, 4945. (b) Rathke, M. W. *Org. Synth. Coll.* **1988**, *6*, 598.
- (16) (a) pK_a of HN(SiMe₃)₂ was determined to be 25.8 in THF: Fraser R. R.; Mansour, T. S.; Savard, S. *J. Org. Chem.* **1985**, *50*, 3232. (b) Acidity of coordinated phosphines can be approximated by using the data on acidity of phosphine oxides: Streitwieser, A.; Juaristi, E. *J. Org. Chem.* **1982**, *47*, 768.
- (17) (a) Rausch, M. D.; Ciappinelli, D. *J. Organomet. Chem.* **1967**, *10*, 127. (b) Chadwick, S. T.; Rennels, R. A.; Rutherford, J. L.; Collum, D. B. *J. Am. Chem. Soc.* **2000**, *122*, 8640.

- (18) (a) (i) O'Donoghue, M. B.; Davis, W. M.; Schrock, R. R. *Inorg. Chem.* **1998**, *37*, 5149. (ii) Freudlich, J. S.; Schrock, R. R.; Davis, W. M. *J. Am. Chem. Soc.* **1996**, *118*, 3643. (iii) Schrock, R. R.; Seidel, S. W.; Schrodi, Y.; Davis, W. M. *Organometallics* **1999**, *18*, 428. (b) Me₃-Si-substituted amines are often used for the introduction of an amido ligand into a Ti coordination sphere, generally accompanied by elimination of Me₃SiCl from a Me₃Si-substituted amine and TiCl₄. For Me₃Si–N vs Ti–Cl metathesis, see: (i) Scollard, J. D.; McConville, H. D.; Payne, N. C.; Vittal, J. J. *Macromolecules* **1996**, *29*, 5241. (ii) Guerin, F.; McConville, H. D.; Payne, N. C. *Organometallics* **1996**, *15*, 5085.
- (19) Fryzuk, M. D.; MacNeil, P. A. *J. Am. Chem. Soc.* **1984**, *106*, 6993.
- (20) Bondi, A. *J. Phys. Chem.* **1964**, *68*, 441.
- (21) (a) Nugent, W. A.; Mayer, J. M. *Metal–Ligand Multiple Bonds*; Wiley: New York, 1988. (b) Cundari, T. R. *Chem. Rev.* **2000**, *100*, 807. (c) Chatt, J.; Falk, C. D.; Leigh, G. J.; Paske, R. J. *J. Chem. Soc. A* **1969**, 2288. (d) Forsellini, E.; Casellato, U.; Graziani, R.; Magon, L. *Acta Crystallogr. B* **1982**, *38*, 3081. (e) Neuhaus, A.; Veldkamp, A.; Frenking G. *Inorg. Chem.* **1994**, *33*, 5278. (f) Abram, U.; Lang, E. S.; Abram, S.; Wegmann, J.; Dilworth, J. R.; Kirmse, R.; Woollins, J. D. *J. Chem. Soc., Dalton Trans.* **1997**, 623. (g) For Tc nitrido complexes, closely related to **17** and **18**, see: Marchi, A.; Marvelli, L.; Rossi, R.; Magon, L.; Uccelli, L.; Bertolasi, V.; Ferretti, V.; Zanobini, F. *J. Chem. Soc., Dalton Trans.* **1993**, 1281.

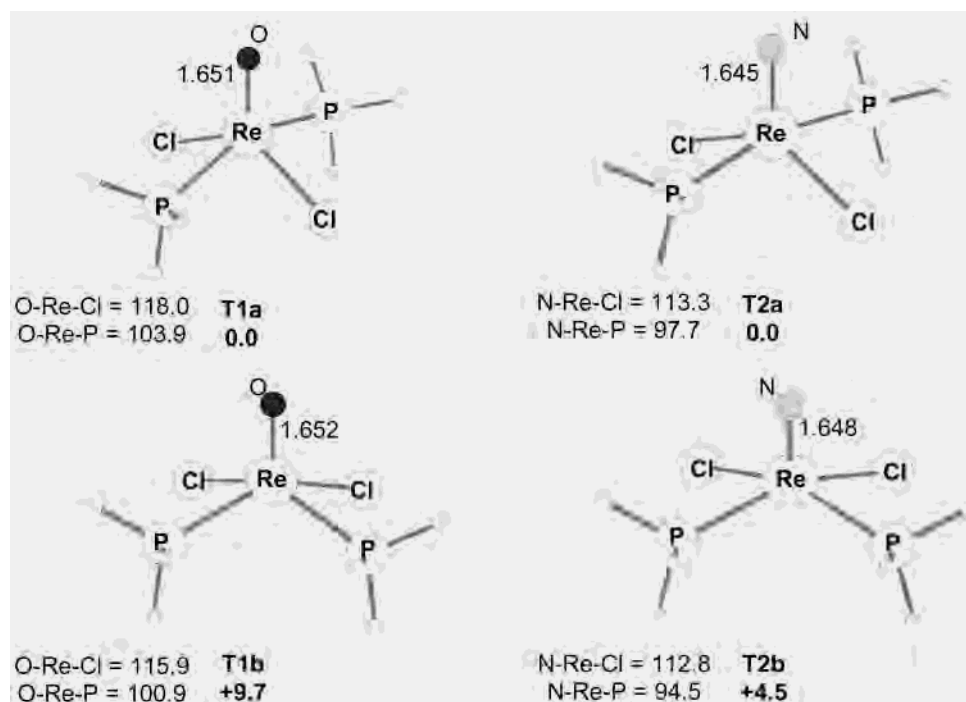


Figure 3. Calculated (DFT) optimized structures and energies (kcal/mol) of isomeric isoelectronic $(\text{H}_3\text{P})_2\text{ReOCl}_2^+$ and $(\text{H}_3\text{P})_2\text{ReNCl}_2$.

The solid-state structure of **18a** shows a different disposition of the ligands about Re (Figure 2). The POP^{Cy} ligand in **18a** adopts a mer geometry. The sum of the angles about the O atom in the structures of both **17b** and **18a** is almost exactly 360° . This is consistent with the sp^2 -hybridized lone pair of the O atom being suitably directed for the interaction with the site trans to the nitrido ligand. However, the $\text{N}-\text{Re}-\text{O}$ angle is closer to 180° in **18a** [$177.56(12)^\circ$] than in **17b** [$165.39(12)^\circ$], and the $\text{Re}-\text{O}$ distance of $2.739(2)$ Å is shorter than in **17b**. This apparently stronger $\text{Re}-\text{O}$ interaction in **18a** as compared to **17b** might be due to the different geometric restrictions imposed by the chelate framework in these structures. The $\text{Re}-\text{N}$ distance of $1.664(2)$ Å in **18a** is slightly longer than that in **17b**, and it might reflect stronger binding of the O trans to the nitrido ligand in **18a**. The key geometric parameters for the structures of **17b** and **18a** are listed in Table 1.

Computational Results

(a) **Monodentate Analogues.** To obtain better insight into the relative stabilities of the species studied experimentally, compounds $[\text{ReOCl}_2(\text{PH}_3)_2]^+$ (**T1**) and $[\text{ReNCl}_2(\text{PH}_3)_2]$ (**T2**) were studied using DFT (B3PW91) methods. This allowed for an examination of the structures and their relative energies when no cyclic strain between the phosphine ligands and no additional interaction ($\text{Re}\cdots\text{O}$ or $\text{Re}\cdots\text{N}$) are present. Both **T1** and **T2** adopt tetragonal pyramidal structures, with the multiply bonded atom (O and N, respectively) occupying the apical site (Figure 3). Two different structures are possible: the phosphine ligands can be either trans to each other (**T1a**, **T2a**) or cis to each other (**T1b**, **T2b**). The structures of **T1** and **T2** are very similar. The $\text{Re}-\text{O}$ and $\text{Re}-\text{N}$ bonds differ by less than 0.01 Å (1.645 vs 1.651 Å). The angles between the apical ligand and the basal ligands

Table 1. Selected Bond Distances and Angles in the Crystallographically Determined Structures of **17b** and **18a** and in the Calculated Optimized (DFT) Structures of **T4b** and **T4c**

	17b , XRD	T4c , DFT	18a , XRD	T4b , DFT
distances, Å				
Re–N	1.651(3)	1.648	1.664(2)	1.643
Re–Cl(Br)1	2.3907(7)	2.428	2.5503(3)	2.423
Re–Cl(Br)2	2.4190(7)	2.428	2.5600(3)	2.434
Re–P1	2.4128(8)	2.392	2.4611(7)	2.417
Re–P2	2.4276(8)	2.392	2.4331(7)	2.417
Re–O	2.856(3)	2.809	2.739(2)	3.013
angles, degrees				
P1–Re–P2	102.97(3)	98.45	162.73(2)	156.78
Cl(Br)1–Re–Cl(Br)2	80.73(3)	85.45	154.209(10)	146.10
N–Re–P1	92.47(9)	95.22	101.31(9)	101.58
N–Re–P2	96.07(9)	95.22	95.92(9)	101.58
N–Re–Cl(Br)1	110.85(9)	109.85	103.40(8)	106.81
N–Re–Cl(Br)2	103.44(9)	109.85	102.39(8)	107.08
N–Re–O	165.39(12)	159.15	177.56(12)	178.08

are slightly larger than 90° and differ by less than 10° in **T1** and **T2**. The isomers with trans phosphines (**T1a**, **T2a**) are C_{2v} -symmetric and more stable than the isomers of C_s symmetry with *cis*-phosphines (**T1b**, $+9.7$ kcal/mol; **T2b**, $+4.5$ kcal/mol). The preference for the trans isomer is twice as large for the oxide **T1a** as for the nitride **T2a**.

(b) **Structures of $[(\text{PNP}^{\text{H}})\text{ReOCl}_2]$ (**T3**) and $[(\text{POP}^{\text{H}})\text{ReNCl}_2]$ (**T4**).** The experimental PNP^{Cy} ligand was modeled as $\text{N}(\text{SiH}_2\text{CH}_2\text{PH}_2)_2$ (PNP^{H}). An analogous model used for the POP^{Cy} ligand was $\text{O}(\text{SiH}_2\text{CH}_2\text{PH}_2)_2$ (POP^{H}). Four structures were examined for both **T3** and **T4**. The **T4** structures can be deduced from the **T3** structures by exchanging O and N. These optimized structures are shown in Figure 4. Because all of these species are isomers, a unique energy reference can be used to compare them.

All **T4** structures are more stable than any **T3** structure, in agreement with experiment. Isomerization of **T3** to **T4**, forming a POP^{H} complex, is thus thermodynamically favored.

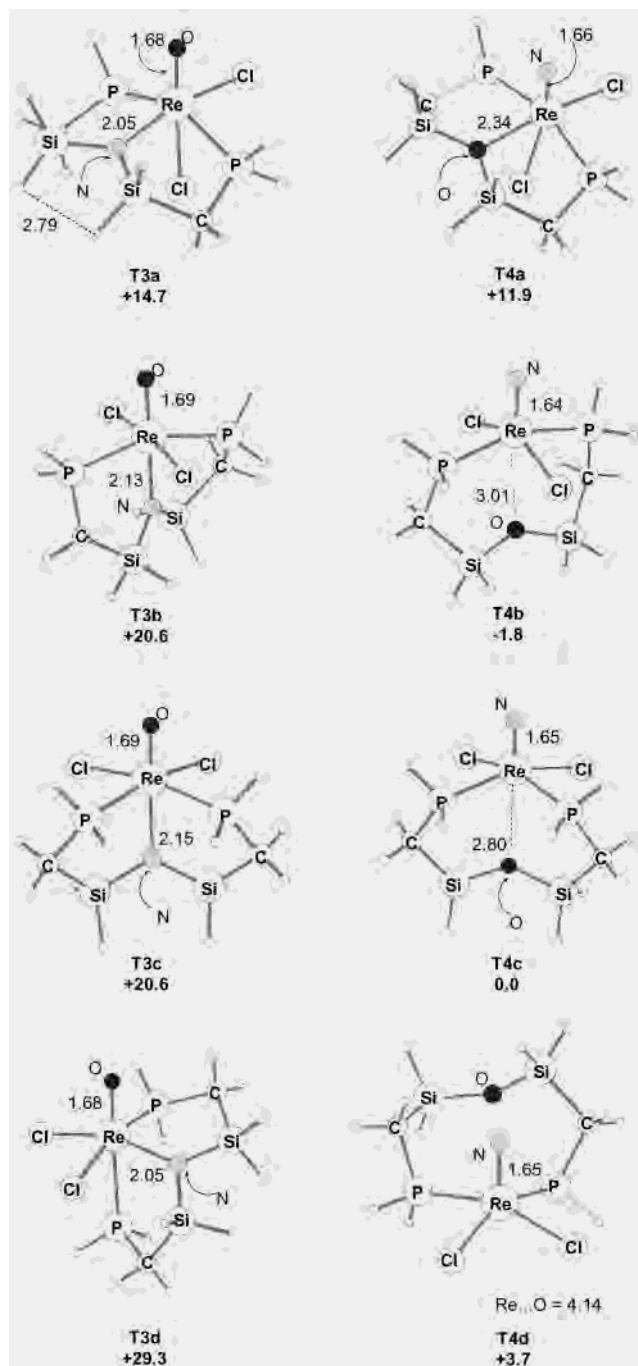


Figure 4. Calculated (DFT) optimized structures and energies (kcal/mol) of isomeric isoenergetic $[(\text{H}_2\text{PCH}_2\text{SiH}_2)_2\text{N}]\text{ReOCl}_2$ and $[\text{H}_2\text{PCH}_2\text{SiH}_2)_2\text{O}]\text{-ReNCl}_2$.

The globally most stable isomer is **T4b** (analogue of **17a**, **18a**), with a mer arrangement of the POP ligand and O trans to the N atom. The $\text{Re}\cdots\text{O}$ distance is very long (3.01 Å), suggesting a very weak interaction of the O with the metal center. The $\text{Re}-\text{O}$ distance is much shorter in **T4a**, yet **T4a** is the least stable **T4** isomer by 13.7 kcal/mol. This shows that the influence of the strength of the $\text{Re}-\text{O}$ bond on the overall stability of the structure is minimal. In contrast, **T3a** (analogue of **14b**, **15b**) is the most stable structure for the **T3** complexes, and it is 5.9 kcal/mol more stable than isomer **T3b** (analogue of **14a**, **15a**). The $\text{Re}-\text{N}$ bond in the **T3** complexes is much shorter than the corresponding $\text{Re}\cdots\text{O}$

distance in the **T4** analogue, whereas the $\text{Re}-\text{O}$ bond in the **T3** species is approximately the same length as the $\text{Re}-\text{N}$ bond in the **T4** species. This shows that the influence of the strength of the $\text{Re}-\text{N}$ bond in **T3** is much stronger than that of $\text{Re}-\text{O}$ in **T4**, as suggested by a simple Lewis structure analysis of these complexes (dative interaction for $\text{Re}\cdots\text{O}$ in **T4** but a single bond in **T3**).

Two isomers were obtained with a fac arrangement of the PNP^{H} (POP^{H}) in **T3** (**T4**). The structures **T3c** and **T4c** (analogue of **17b**, **18b**), with both P atoms trans to Cl, are quasi-isoenergetic with **T3b** and **T4b**, respectively, which shows that structures with a fac arrangement are also energetically accessible. Structure **T3d** has only one P atom trans to Cl; the other phosphine is trans to O. Even though the $\text{Re}-\text{N}$ distance is quite short, **T3d** is a high-energy species. A **T4** analogue of **T3d** with one P trans to N and O interacting trans to Cl could not be found: dissociation of the O atom ($\text{Re}\cdots\text{O} = 4.14$ Å) allows coordination of both P and Cl in the basal sites. Consequently, **T4c** and **T4d** exhibit similar coordinations, except that O interacts with the vacant site in **T4c** and not in **T4d**. The energy difference between these two species can thus be used to evaluate the strength of the $\text{Re}\cdots\text{O}$ interaction when it is trans to N. Because **T4c** is only 3.7 kcal/mol more stable than **T4d**, this feature confirms the hypothesis of a very weak $\text{Re}\cdots\text{O}$ interaction.

(c) Rationale for Structural Preferences. The basic structures of the monodentate complexes **T1** and **T2** show a modest preference for the trans arrangement of the phosphines; yet **T3b** and **T3c** are isoenergetic, and **T4b** and **T4c** are likewise isoenergetic. This indicates that the PXP^{H} backbone ($\text{X} = \text{N}, \text{O}$) favors the fac geometry.

The most important factor determining the relative stabilities of the isomers of **T3** and **T4** structures is the strong trans influence of the oxo or nitrido ligand.²¹ A bond to a ligand trans to oxo or nitrido will be considerably weakened. This is evident from the fact that, in all cases, the bond to a donor atom trans to an oxo or a nitrido group is substantially longer than an analogous bond in an equatorial position. Therefore, those structures should be more stable that have the weakest ligand trans to a multiply bonded atom. In a sense, the bond to such a ligand is sacrificed to the strong trans influence ligand so that the bonds to other ligands have the opportunity to contribute the greatest thermodynamic gain. For the **T3** series, the best “sacrificial” ligand is the chloride; the **T3a** structure is the most stable. For the **T4** series the coordination of the weakest ligand, the Si–O–Si oxygen, trans to the nitrido group gives more stable structures. Indeed, equivalents of **T4b** (**17a**, **18a**) and **T4c** (**17b**, **18b**) are the structures observed experimentally.^{21g} The analogues of **T3a** (**14b**, **15b**) and **T3b** (**14a**, **15a**) are the two isomers observed in the experiment for the Re oxo compounds. It should be noted, however, that the introduction of real alkyl substituents on the PNP ligand instead of the model Hs will destabilize the **T3a** (repulsion between eclipsed Si–Me groups) and the **T3c** (cis C_2P groups) structures. Thus, PNP^{Cy} analogues of **T3a** and **T3b** should

be closer in energy and more stable than **T3c**, in accord with the experimental observations.

(d) Correlation with the Experimental Results. The computed structures **T4b** and **T4c** correlate closely with the experimental results of the X-ray diffraction studies of **18a** and **17b**, respectively (see Table 1). Slight differences in the geometrical parameters can be ascribed to steric factors, which are absent in the theoretical model. The somewhat greater differences in the Re–O bond distances between theory and experiment occur because any very weak bonding (e.g., Re–O) is more difficult to model accurately with DFT.

On the basis of the structural and computational studies, it is easy to understand why Et_3P reacts much faster with the **T4c**-type structures (**17b**, **18b**) than with the **T4b**-type structures (**17a**, **18a**). The oxygen atom is coordinated weakly in both cases, and presumably, the barrier to its dissociation is negligible. However, in the **T4c**-type structure, oxygen dissociation (giving a **T4d** structure) can lead to a sterically available empty site, whereas in the **T4b**-type structure, even with the oxygen dissociated, the backbone of the POP ligand will block access to the empty site. Moreover, X-ray data (vide supra) support a stronger Re–O interaction in **18a** than in **17b**. Et_3P can easily bind to the empty site of a **T4d** structure, facilitating the loss of the POP ligand. To create an available empty site, **T4b** would have to dissociate a phosphine arm first, clearly a higher activation barrier process than dissociation of the weakly bound disilyl ether moiety. From the thermodynamic point of view, apparently having three phosphine donors in **22** or **23** is preferred to having two phosphine donors and a weak donor ether in **17** and **18**, despite the unfavorable entropy change.

Conclusion

This paper began with the assertion that those bonds that are conveniently formed in ligand syntheses might be, for the same reason (e.g., polarity), vulnerable to attack once they are incorporated into a metal complex.²² Because the reaction times and temperatures employed in this report are relatively extreme, the message of this work is not altogether pessimistic: chemical reactivity that proceeds at or below 25 °C or in a short period of time at elevated temperature is both attractive and realizable without rearrangement of the ligand backbone. Nevertheless, the reactions reported here are interesting, and even surprising at first sight, because of the extensive rearrangement of the molecules. The idea that oxide or halide ligands can be nucleophiles for internal “displacement” warrants attention.

Experimental Section

General Considerations. All manipulations were performed using standard Schlenk techniques or an argon-filled glovebox unless otherwise noted. Solvents were distilled from Na/benzophenone or CaH_2 , as appropriate. $\text{LiN}(\text{SiMe}_2\text{CH}_2\text{PCy}_2)_2 \cdot \text{Et}_2\text{O}$ (**1a**) and $\text{HN}(\text{SiMe}_2\text{CH}_2\text{PCy}_2)_2$ were prepared by modification of established procedures.¹ All other reagents were used as received from commercial vendors. ^1H NMR chemical shifts are reported in ppm relative to protio impurities in the deuterated solvents. ^{31}P spectra are referenced to external standards of 85% H_3PO_4 (at 0 ppm). NMR spectra were recorded with a Varian Gemini 2000 instrument (300 MHz ^1H , 121 MHz ^{31}P , 75 MHz ^{13}C), a Varian Unity Inova

instrument (400 MHz ^1H , 162 MHz ^{31}P , 101 MHz ^{13}C , 59 MHz ^6Li), or a Varian Unity Inova instrument (500 MHz ^1H , 126 MHz ^{13}C). GC-MS spectra were recorded on a Hewlett-Packard 5890/5971 series GC-MS.

Computational Details. The calculations were carried out using the Gaussian 98 set of programs²³ within the framework of DFT at the B3PW91 level of the theory.^{24a,b} Re was represented using the Hay–Wadt relativistic electron core potential for the 46 innermost electrons and its associated basis set.^{24c} Si, P, and Cl were also represented with the Los Alamos ECPs and their associated basis set,²⁵ completed by an additional d polarization function.²⁶ The 6-31G** basis set was used for H, C, N, and O.²⁷ Full geometry optimizations without symmetry constraints were carried out using the default algorithm. The nature of all minima was checked by analytical frequencies calculation. Evaluation of the Gibbs energy was done using the frequency calculation results and does not affect the relative stabilities of the various species. Results are thus given in term of nuclear plus electronic energies.

Preparation of 1–3. (PNP^{Cy})Li·Et₂O (1a). Cy_2PH (11.0 mL, 54.4 mmol) was dissolved in 100 mL of THF. To this solution was added *n*-BuLi in hexanes (34.0 mL of 1.6 M solution, 54.4 mmol), which caused the appearance of the yellow color of $\text{Cy}_2\text{-PLi}$. The solution was stirred for 15 min, and then $(\text{ClCH}_2\text{SiMe}_2)_2\text{-NH}$ (3.95 mL, 18.1 mmol) was added via syringe. The mixture was stirred for 15 min, during which it became practically colorless. Another portion of *n*-BuLi (11.3 mL of 1.6 M solution, 18.1 mmol) was added, the mixture turned yellow and was stirred for 15 min, and then $(\text{ClCH}_2\text{SiMe}_2)_2\text{-NH}$ (1.32 mL, 6.04 mmol) was added via syringe. The mixture was stirred for 15 min, and then the third portion of *n*-BuLi (3.80 mL of 1.6 M solution, 6.04 mmol) was added; the mixture turned yellow and was stirred for 15 min, and then $(\text{ClCH}_2\text{SiMe}_2)_2\text{-NH}$ (0.44 mL, 2.0 mmol) was added via syringe. The mixture was stirred for 15 min, the volatiles were removed, and the residue was twice triturated with heptane. Then, it was extracted with pentane and filtered. The filtrate was stripped to dryness, triturated with heptane, extracted with pentane, and filtered. The filtrate was stripped to dryness. The residue was then crystallized from ether at –30 °C, producing three fractions totaling 12.9 g (74%) of pure product. For the preparation of the sodium salt **2**, the combined washings and supernatants were treated with NaOCMe_2Et (0.66 g, 6.0 mmol) in benzene/pentane (20 mL) and

- (22) Giesbrecht, G. R.; Shafir, A.; Arnold, J. *Chem. Commun.* **2000**, 2135.
 (23) Frisch, M. J.; Trucks, G. W.; Schlegel, H. B.; Scuseria, G. E.; Robb, M. A.; Cheeseman, J. R.; Zakrzewski, V. G.; Montgomery, J. A., Jr.; Stratmann, R. E.; Burant, J. C.; Dapprich, S.; Millam, J. M.; Daniels, A. D.; Kudin, K. N.; Strain, M. C.; Farkas, O.; Tomasi, J.; Barone, V.; Cossi, M.; Cammi, R.; Mennucci, B.; Pomelli, C.; Adamo, C.; Clifford, S.; Ochterski, J.; Petersson, G. A.; Ayala, P. Y.; Cui, Q.; Morokuma, K.; Malick, D. K.; Rabuck, A. D.; Raghavachari, K.; Foresman, J. B.; Cioslowski, J.; Ortiz, J. V.; Baboul, A. G.; Stefanov, B. B.; Liu, G.; Liashenko, A.; Piskorz, P.; Komaromi, I.; Gomperts, R.; Martin, R. L.; Fox, D. J.; Keith, T.; Al-Laham, M. A.; Peng, C. Y.; Nanayakkara, A.; Gonzalez, C.; Challacombe, M.; Gill, P. M. W.; Johnson, B.; Chen, W.; Wong, M. W.; Andres, J. L.; Gonzalez; Head-Gordon, M.; Replogle, E. S.; Pople, J. A. *Gaussian 98*, revision A.7; Gaussian, Inc.: Pittsburgh, PA, 1998.
 (24) (a) Becke, A. D. *J. Chem. Phys.* **1993**, *98*, 5648. (b) Perdew, J. P.; Wang, Y. *Phys. Rev. B* **1992**, *45*, 13244. (c) Hay, P. G.; Wadt, W. R. *J. Chem. Phys.* **1985**, *82*, 299.
 (25) Wadt, W. R.; Hay, P. G. *J. Chem. Phys.* **1985**, *82*, 184.
 (26) Höllwarth, A. H.; Böhme, M. B.; Dapprich, S.; Ehlers, A. W.; Gobbi, A.; Jonas, V.; Köhler, K. F.; Stegman, R.; Veldkamp, A.; Frenking, G. *Chem. Phys. Lett.* **1993**, *208*, 237.
 (27) Hariharan, P. C.; Pople, J. A. *Theor. Chem. Acta* **1973**, *28*, 213.
 (28) Albers, M. O.; Ashworth, T. V.; Oosthuisen, H. E.; Singleton, E. *Inorg. Synth.* **1987**, *26*, 68.
 (29) ORTEP-3 for Windows; Farrugia, L. J. *J. Appl. Crystallogr.* **1993**, *30*, 565.

allowed to stand for 48 h. A colorless crystalline precipitate of (PNP^{Cy})Na formed over this time. It was separated by decantation, washed with benzene, and dried in vacuo to give 0.75 g (5% based on the initial amount of Cy₂PH). (PNP^{Cy})Na can also be obtained as a crystalline precipitate from equimolar amounts of (PNP^{Cy})Li and NaOCMe₂Et in benzene in >75% yield. ¹H NMR (C₆D₆): δ 0.50 (s, 12H, SiMe₂), δ 0.78 (d, *J*_{PH} = 4 Hz, 4H, CH₂), δ 1.12 [t, 4.5H, ³*J*_{HH} = 7 Hz, O(CH₂CH₃)₂], δ 1.26 [br m, 20H, P(C₆H₁₁)₂], δ 1.64 [br t, 8H, *J*_{HH} = 12 Hz, P(C₆H₁₁)₂], δ 1.77 [br s, 8H, P(C₆H₁₁)₂], δ 1.90 [br s, 8H, P(C₆H₁₁)₂], δ 3.30 [q, 3H, ³*J*_{HH} = 7 Hz, O(CH₂CH₃)₂]. ¹³C{¹H} NMR (101 MHz, C₆D₆, 20 °C): δ 7.3 (s, SiMe₂), δ 11.4 (d, *J*_{PC} = 24 Hz, CH₂), δ 15.4 [s, O(CH₂CH₃)₂], δ 26.9 [s, P(4-C₆H₁₁)₂], δ 27.9 [d, *J*_{PC} = 9 Hz, P(3/5-C₆H₁₁)₂], δ 28.0 [d, *J*_{PC} = 9 Hz, P(3/5-C₆H₁₁)₂], δ 30.3 [d, *J*_{PC} = 9 Hz, P(2/6-C₆H₁₁)₂], δ 30.6 [d, *J*_{PC} = 9 Hz, P(2/6-C₆H₁₁)₂], δ 34.4 [br s, P(1-C₆H₁₁)₂], δ 65.8 [s, O(CH₂CH₃)₂]. ³¹P{¹H} NMR (C₆D₆): δ -9.3 (very br s).

(PNP^{Cy})Li·TMEDA (**1b**). (PNP^{Cy})Li·TMEDA (**1b**) can be obtained by recrystallizing (PNP^{Cy})Li·Et₂O (**1a**) from ether or pentane in the presence of >1 equiv of TMEDA. ¹H NMR (C₆D₆): δ 2.07 (br s, 12H, NCH₃), 1.94 (br s, 4H, NCH₂), 1.6–2.0 (several multiplets, 20H, Cy), 1.10–1.40 (several multiplets, 20H, Cy), 0.78 (br s, 4H, PCH₂Si), 0.50 (s, 12H, SiCH₃). ¹³C NMR (C₆D₆): δ 57.2 (s, TMEDA), 46.6 (s, TMEDA), 34.8 (d, *J* = 10 Hz, P–CH), 30.7 (d, *J* = 10 Hz, CH₂ of Cy), 30.4 (d, *J* = 10 Hz, CH₂ of Cy), 28.0 (d, *J* = 9 Hz, CH₂ of Cy), 27.8 (d, *J* = 9 Hz, CH₂ of Cy), 27.1 (s, CH₂ of Cy). ³¹P NMR (C₆D₆): δ -7.9 (br s).

(PNP^{Cy})Na (**2**). ¹H NMR (C₆D₆): δ 1.0–2.1 (several broad multiplets, 40H, Cy), 0.80 (br s, 4H, PCH₂Si), 0.51 (s, 12H, SiCH₃). ³¹P NMR (C₆D₆): δ -12.1 (br s).

(PNP^{Cy})K (**3**). **3** was prepared in situ by an exchange reaction in C₆D₆ between **1b** (13.5 mg, 20 μmol) and potassium menthoxide (3.9 mg, 20 μmol). ¹H NMR (C₆D₆), selected resonances: δ 0.79 (d, 3 Hz, 4H, PCH₂Si), 0.44 (s, 12H, SiCH₃). ³¹P NMR (C₆D₆): δ -8.6 (s).

(PNP^{Cy})MgBr·0.75THF·0.25dioxane (**5**) [Attempted Preparation of (PNP^{Cy})₂Mg]. (PNP^{Cy})Na (1.22 g, 2.12 mmol) was dissolved in 20 mL of THF/Et₂O and MgBr₂·Et₂O (0.280 g, 1.06 mmol) was added. The mixture was stirred for 2 h, and then 0.5 mL of 1,4-dioxane was added. The mixture was stirred for 1 h, and then the volatiles were removed. The residue was extracted with ether and filtered. The filtrate was stripped, and the white residue was recrystallized from ether/pentane at -30 °C to give 0.62 g (0.85 mmol, 40%) of (PNP^{Cy})MgBr·0.75THF·0.25dioxane. ¹H NMR (C₆D₆): δ 3.76 (br, 3H, THF), 3.37 (s, 2H, 1,4-dioxane), 1.85 (br t, 8H, Cy), 1.50–1.75 (m, 16H, Cy), 1.10–1.45 (several multiplets, 19H, Cy and THF), 0.73 (d, *J* = 10 Hz, P–CH₂–Si), 0.40 (s, 12H, SiCH₃). ³¹P NMR (C₆D₆): δ -12.5 (s).

(PNP^{Cy})Ag (**6**). (PNP^{Cy})Na (0.700 g, 2.22 mmol) was dissolved in 20 mL of THF, and AgOTf (0.310 g, 1.22 mmol) was added. The mixture was stirred in the dark for 3 h, and then the volatiles were removed. The residue was extracted with ether and filtered to remove NaOTf. The filtrate was stripped, and the white residue was recrystallized from ether/pentane at -30 °C to give 0.60 g (75%) of (PNP^{Cy})Ag. ¹H NMR (C₆D₆): δ 1.78–1.88 (br dd, 8H, Cy), 1.49–1.71 (several multiplets, 16H, Cy), 0.98–1.34 (several multiplets, 20H, Cy), 0.92 (m, 4H, PCH₂Si), 0.53 (s, 12H, SiCH₃). ¹³C NMR (C₆D₆): δ 34.1 (q, *J* = 5 Hz, P–CH), 30.8 (br, CH₂ of Cy), 30.0 (br, CH₂ of Cy), 27.15–27.50 (m, CH₂ of Cy), 26.5 (br s, CH₂ of Cy), 13.8 (br s, PCH₂Si), 7.5 (s, SiCH₃). ³¹P NMR (C₆D₆): δ 19.4 (two doublets, *J*_{PAG} = 434 and 500 Hz).

(PNP^{Cy})ReOCl₂ (**14**). Method 1 [from (Ph₃PO)(Me₂S)ReOCl₃]⁷ (**12**). (PNP^{Cy})Li (**1a**) (0.930 g, 1.47 mmol) and (Ph₃-

PO)(Me₂S)ReOCl₃ (0.975 g, 1.50 mmol) were placed in a flask and treated with 50 mL of benzene. The reaction mixture was stirred for 18 h, and then the volatiles were removed under vacuum. The residue was triturated with heptane, extracted with pentane, and filtered. The filtrate was stripped to dryness and treated with 10 mL of cold Et₂O, and the flask was stored in a freezer at -30 °C for 3 h. Then, the supernatant was carefully decanted, and the green residue was washed with cold Et₂O and pentane and dried in vacuo to give 0.480 g (40%) of the product. The combined washings were stripped to dryness and treated analogously to give the second crop of the product, 0.200 g (16%). Alternatively, the product can be obtained by crystallization from various ether/pentane mixtures at low temperature. The product is obtained as a mixture of C_{2v} and C_s isomers; the ratio is poorly reproducible and is dependent on the handling history.

Method 2 [from (Ph₃PO)₂ReOCl₃ (**10**)].⁶ (PNP^{Cy})Li (**1a**) (0.950 g, 1.50 mmol) and (Ph₃PO)₂ReOCl₃ (1.250 g, 1.50 mmol) were placed in a flask and treated with 25 mL of benzene. The reaction mixture was stirred for 5.5 h. During this time, the mixture became dark green. Elemental sulfur (0.112 g, 3.50 mmol) was added to the reaction mixture. It was stirred at ambient temperature for 18 h and then for 10 min at 55 °C. The volatiles were then removed under vacuum, and the residue was triturated with heptane, extracted with pentane, and filtered. The filtrate was stripped to dryness, extracted with pentane, and filtered again. From this solution, 0.84 g (70%) of the product was obtained in the same manner as described for method 1.

C_{2v} Isomer (**14a**). ¹H NMR (C₆D₆): δ 2.54 (br t, 4H, Cy), 2.43 (br d, *J* = 11 Hz, 4H, Cy), 2.02 (br d, *J* = 13 Hz, 4H, Cy), 1.71 (br d, *J* = 12 Hz, 8H, Cy), 1.05–1.60 (several multiplets, 28H, Cy and PCH₂Si), 0.27 (s, 12H, SiCH₃). ¹³C NMR (C₆D₆): δ 36.9 (t, *J* = 10 Hz, P–CH), 29.3 (br s, CH₂ of Cy), 29.2 (br s, CH₂ of Cy), 27.7 (br t, *J* = 5 Hz, CH₂ of Cy), 27.6 (br t, *J* = 6 Hz, CH₂ of Cy), 26.6 (br s, CH₂ of Cy), 10.6 (br t, *J* = 6 Hz, PCH₂Si), 5.2 (br s, SiCH₃). ³¹P NMR (C₆D₆): δ 8.9 (s).

C_s Isomer (**14b**). ¹H NMR (C₆D₆): δ 2.98 (br d, *J* = 11 Hz, 2H, Cy), 2.83 (m, 2H, Cy), 2.14–2.24 (m, 6H, Cy), 2.06 (br d, *J* = 12 Hz, 2H, Cy), 1.69 (br, 4H, Cy), 1.63 (br d, *J* = 12 Hz, 4H, Cy), 0.95–1.57 (several multiplets, 26H, Cy and PCH₂Si), 0.80 (dvt, ²*J*_{HH} = 14 Hz, *J*_{PH} = 7 Hz, 2H, PCH₂Si), 0.56 (s, 6H, SiCH₃), 0.30 (s, 6H, SiCH₃). ¹³C NMR (C₆D₆): δ 37.7 (t, *J* = 13 Hz, P–CH), 36.7 (t, *J* = 9 Hz, P–CH), 28.62 (br s, CH₂ of Cy), 28.58 (br s, CH₂ of Cy), 28.5 (br s, CH₂ of Cy), 28.4 (br s, CH₂ of Cy), 27.8 (br t, *J* = 5 Hz, CH₂ of Cy), 27.8 (2 overlapping t, *J* = 5 Hz, CH₂ of Cy), 27.3 (br t, *J* = 5 Hz, CH₂ of Cy), 26.6 (br s, CH₂ of Cy), 26.4 (br s, CH₂ of Cy), 12.2 (br s, P–CH₂–Si), 5.1 (br s, SiCH₃), 4.7 (br s, SiCH₃). ³¹P NMR (C₆D₆): δ -0.4 (s). Elem anal (mixture of isomers). Calcd for C₃₀H₆₀Cl₂NP₂ReSi₂·0.5C₄H₁₀O: C, 44.53; H, 7.59; N, 1.62. Found: C, 44.58; H, 7.53; N, 1.62.

(PNP^{Cy})ReOBr₂ (**15**). (PNP^{Cy})ReOBr₂ was synthesized analogously to (PNP^{Cy})ReOCl₂ (**14**), and obtained in similar yields, using (Ph₃PO)(Me₂S)ReOBr₃ (**13**)⁷ or (Ph₃PO)₂ReOBr₃ (**11**)⁶ as the Re source. All samples of (PNP^{Cy})ReOBr₂ appear as ca. 1:1 mixture of isomers when dissolved in C₆D₆ at ambient temperature.

C_{2v} Isomer (**15a**). ¹H NMR (C₆D₆), selected resonances: δ 0.22 (s, 12H, SiCH₃). ¹³C NMR (C₆D₆): δ 37.9 (t, *J* = 11 Hz, P–CH), 29.6 (br s, CH₂ of Cy), 29.4 (br s, CH₂ of Cy), 27.8 (br t, CH₂ of Cy), 26.7 (br s, CH₂ of Cy), 12.5 (t, *J* = 7 Hz, PCH₂Si), 5.1 (br s, SiCH₃). ³¹P NMR (C₆D₆): δ 6.6 (s).

C_s Isomer (**15b**). ¹H NMR (C₆D₆), selected resonances: δ 0.57 (s, 6H, SiCH₃), 0.26 (s, 6H, SiCH₃). ¹³C NMR (C₆D₆): δ 39.0 (t, *J* = 13 Hz, P–CH), 37.8 (t, P–CH), 29.4 (br s, CH₂ of Cy), 29.3 (br s, CH₂ of Cy), 28.9 (br s, CH₂ of Cy), 28.8 (br s, CH₂ of Cy),

27.2–28.0 (4 triplets, CH_2 of Cy), 26.6 (br s, CH_2 of Cy), 26.4 (br s, CH_2 of Cy), 13.2 (br t, PCH_2Si), 4.5 (br s, SiCH_3). ^{31}P NMR (C_6D_6): δ -3.5 (s).

(PNP^{Cy}) ReOBrCl (**16**). (PNP^{Cy}) MgBr (**5**) (19.5 mg, 32.0 μmol) and (Ph_3PO)(Me_2S) ReOCl_3 (**12**)⁷ (21.1 mg, 32.0 μmol) were mixed in C_6D_6 and allowed to react for 10 h. The distribution of products was analyzed by NMR spectroscopy. Alternatively, (PNP^{Cy}) ReOBrCl can be observed by treating (PNP^{Cy}) ReOCl_2 with $\text{MgBr}_2 \cdot \text{Et}_2\text{O}$ in C_6D_6 . Three isomers of **16** were observed by ^{31}P NMR (C_6D_6): δ 6.9 (s), -0.7 (s), -6.1 (s).

(POP^{Cy}) ReNCl_2 (**17**). Both isomers can be observed in situ by heating <30 mg samples of (PNP^{Cy}) ReOCl_2 (**14**) in 0.6 mL of C_6D_6 for 24 h at 90 °C. (POP^{Cy}) ReNCl_2 (C_{2v}) (**17a**). Solid (PNP^{Cy}) ReOCl_2 (**14**) (9.0 mg, 11 μmol) was placed into a J. Young tube. The tube was placed into a 115 °C oil bath and was kept at this temperature for 5 days. During this time, the solid changed color from green to orange. The solid was then dissolved in C_6D_6 , and the NMR analysis showed ca. 95% conversion to exclusively (POP^{Cy}) ReNCl_2 (C_{2v}) (**17a**). However, after 2 days at ambient temperature in solution, signals of the C_s isomer appeared as well. ^1H NMR (C_6D_6): δ 2.76 (m, 8H, Cy), 1.93 (br d, $J = 12$ Hz, 4H, Cy), 1.72 (br d, 8H, $J = 11$ Hz, Cy), 1.07–1.62 (several multiplets, 28H, Cy and PCH_2Si), 0.14 (s, 12H, SiCH_3). ^{13}C NMR (C_6D_6): δ 33.8 (t, $J = 12$ Hz, $\text{P}-\text{CH}$), 30.2 (d, $J = 15$ Hz, CH_2 of Cy), 29.2 (br s, CH_2 of Cy), 28.2 (br t, $J = 5$ Hz, CH_2 of Cy), 27.9 (br t, $J = 5$ Hz, CH_2 of Cy), 26.9 (br s, CH_2 of Cy), 10.2 (br t, $\text{P}-\text{CH}_2-\text{Si}$), 2.7 (br s, SiCH_3). ^{31}P NMR (C_6D_6): δ 18.9 (s).

(POP^{Cy}) ReNCl_2 (C_s) (**17b**). (PNP^{Cy}) ReOCl_2 (**14**) (100 mg, 120 μmol) was dissolved in 0.7 mL of C_6D_6 and heated for 24 h at 90 °C. During this time, yellow X-ray-quality crystals of (POP^{Cy}) ReNCl_2 (C_s) (**17b**) precipitated out of the brown-orange solution. These crystals were separated by filtration, washed with pentane, and dried. Yield: 45 mg (45%). The supernatant contained mostly (POP^{Cy}) ReNCl_2 (C_{2v}) (**17a**). ^1H NMR (C_6D_6): δ 2.81 (br, 2H, Cy), 2.58 (br, 2H, Cy), 2.27 (br, Cy), 1.47–2.1 (several multiplets, 26H, Cy), 0.9–1.3 (several multiplets, 16H, Cy and PCH_2Si), 0.81 (t, $J = 14$ Hz, 2H, PCH_2Si), 0.37 (s, 6H, SiCH_3), -0.05 (s, 6H, SiCH_3). ^{31}P NMR (C_6D_6): δ 18.6 (s).

(POP^{Cy}) ReNBr_2 (**18**). Both isomers can be observed in situ by heating <30-mg samples of (PNP^{Cy}) ReOBr_2 (**15**) in 0.6 mL of C_6D_6 for 24 h at 90 °C.

(POP^{Cy}) ReNBr_2 (C_{2v}) (**18a**). (PNP^{Cy}) ReOBr_2 (**15**) (370 mg, 405 μmol) was dissolved in 3 mL of toluene and was heated for 24 h at 90 °C. During this time, the color changed from green to orange. A small amount of insolubles was filtered off, and the reaction vessel was additionally rinsed with a small amount of benzene and filtered. The combined filtrates, ca. 5 mL, were layered with 5 mL of pentane and allowed to stand at ambient temperature for 2 days. Orange X-ray-quality crystals of (POP^{Cy}) ReNBr_2 (C_{2v}) (**18a**) precipitated. They were washed with pentane and dried to give 0.220 g (55%) of pure product. The combined washings and the supernatant were cooled to -30 °C for 2 days. The second crop of crystals precipitated (0.140 g, 35%). The isolated crystals contained 1 equiv of benzene per Re. A solvent-free sample could be prepared by recrystallization from CH_2Cl_2 /pentane at low temperature and prolonged drying under vacuum. ^1H NMR (C_6D_6): δ 3.06 (br t, 4H, Cy), 2.79 (br d, 4H, $J = 11$ Hz, Cy), 1.91 (br d, $J = 13$ Hz, 4H, Cy), 1.72 (br d, 8H, $J = 11$ Hz, Cy), 1.40–1.65 (several multiplets, 20H, Cy), 1.1–1.3 (several multiplets, 8H, Cy and PCH_2-Si), 0.13 (s, 12H, SiCH_3). ^{13}C NMR (C_6D_6): δ 34.6 (t, $J = 12$ Hz, $\text{P}-\text{CH}$), 30.3 (br s, CH_2 of Cy), 29.4 (br s, CH_2 of Cy), 28.1 (br t, $J = 5$ Hz, CH_2 of Cy), 28.0 (br t, $J = 5$ Hz, CH_2 of Cy), 26.9 (br s, CH_2 of Cy), 11.1 (br, $\text{P}-\text{CH}_2-\text{Si}$), 2.9 (br s, SiCH_3). ^{31}P NMR

(C_6D_6): δ 15.1 (s). Elem anal. Calcd for $\text{C}_{30}\text{H}_{60}\text{Br}_2\text{NP}_2\text{ReSi}_2 \cdot 0.25\text{C}_5\text{H}_{12}$: C, 40.23; H, 6.80; N, 1.50. Found: C, 40.09; H, 6.90; N, 1.53.

(POP^{Cy}) ReNBr_2 (C_s) (**18b**). We were unable to isolate the pure C_s isomer, so we report only partial NMR data from observations of the mixture of isomers in situ. ^1H NMR (C_6D_6), selected resonances: δ 0.34 (s, 12H, SiCH_3), -0.06 (s, 12H, SiCH_3). ^{31}P NMR (C_6D_6): δ 16.7 (s).

($\text{POP}^{\text{Cy}}-\text{Cl}$) ReNCiMe (**20**). **20a** and **20b** can be observed in situ upon prolonged (> 2 days) heating of **14** or **17** C_6D_6 solutions at 90 °C.

Major Isomer. ^1H NMR (C_6D_6): 2.81 (br, 2H, Cy), 2.58 (br, 2H, Cy), 2.27 (br, Cy), 1.47–2.1 (several multiplets, 26H, Cy), 0.9–1.3 (several multiplets, 16H, Cy and PCH_2Si), 0.81 (t, $J = 14$ Hz, 2H, PCH_2Si), 0.37 (s, 6H, SiCH_3), -0.05 (s, 6H, SiCH_3). ^{13}C NMR (C_6D_6): δ -14.8 (t, $J_{\text{CP}} = 5.5$ Hz, $\text{Re}-\text{CH}_3$). ^{31}P NMR (C_6D_6): δ AB system ($J_{\text{PP}} = 168$ Hz): 24.7 (d), 22.8 (d).

Minor Isomer. ^1H NMR (C_6D_6), selected resonances: δ 0.39 (s, 3H, SiMe), 0.38 (s, 3H, SiMe), 0.07 (s, 3H, SiMe). ^{13}C NMR (C_6D_6), selected resonances: δ -15.5 (t, $J_{\text{CP}} = 5.5$ Hz, $\text{Re}-\text{CH}_3$). ^{31}P NMR (C_6D_6): δ AB system ($J_{\text{PP}} = 166$ Hz) 24.8 (d), 22.7 (d).

($\text{POP}^{\text{Cy}}-\text{Br}$) ReNBrMe (**21**). **21** can be observed in situ upon prolonged (> 2 days) heating of **15** or **18** C_6D_6 solutions at 90 °C. Only a small fraction of **21** is present in the mixture (ca. 5%), and further heating does not improve the conversion. Only one isomer can be reliably observed in the ^{31}P NMR spectrum; ^1H NMR resonances are obstructed by **18a** and **18b** and cannot be assigned. ^{31}P NMR (C_6D_6): δ AB system ($J_{\text{PP}} = 162$ Hz) 22.5 (d), 21.2 (d).

POP^{Cy} (**24**), [(Et_3P) 3ReNCl_2] (**22**),¹⁰ [(Et_3P) 3ReNBr_2] (**23**). Upon codissolution of a sample of a mixture of isomers of [(POP^{Cy}) ReNCl_2] (**17**) with an excess (> 3 equiv) of Et_3P in C_6D_6 at ambient temperature, the signals due to **17b** disappear, and POP^{Cy} (**24**) along with [(Et_3P) 3ReNCl_2] (**22**) can be observed. Further heating of the mixture for 10 h at 80 °C results in full conversion of **17a** to **22** and **24**. The same results are obtained upon heating **14** with an excess of Et_3P for 24 h at 80 °C. The dibromo analogues **23** and **24** can be prepared in the same manner starting either from **15** or **18**. The solids derived from resulting solutions were analyzed by mass spectrometry (EI).

POP^{Cy} (**24**). ^1H NMR (C_6D_6), selected resonances: δ 0.37 (s, 12H, SiMe), 0.69 (d, 4H, $J = 2.5$ Hz, SiCH_2P). ^{31}P NMR (C_6D_6): δ -13.0 (s). MS (EI): 471 ($\text{M}^+ - \text{Cy}$), 388 ($\text{M}^+ - 2\text{Cy}$).

[(Et_3P) 3ReNCl_2] (**22**). ^1H NMR (C_6D_6): δ 2.28 (m, 6H, PCH_2), 2.03 (pseudo quintet, $J = 8$ Hz, 6H, PCH_2), 1.93 (m, 6H, PCH_2), 1.11 (pseudo quintet, 18H, PCH_2CH_3), 1.02 (dt, 9H, $J_{\text{PH}} = 14$ Hz, $J_{\text{HH}} = 8$ Hz, PCH_2CH_3). ^{31}P NMR (C_6D_6): δ -4.8 (d, $J = 15.5$ Hz), -12.7 (t, $J = 15.5$ Hz). MS (EI): 505, 507, 509 ($\text{M}^+ - \text{Et}_3\text{P}$), 387, 389, 391 ($\text{M}^+ - 2\text{Et}_3\text{P}$), 118 (Et_3P^+).

[(Et_3P) 3ReNBr_2] (**23**). ^1H NMR (C_6D_6): δ 2.40 (m, 6H, PCH_2), 2.09 (pseudo quintet, $J = 8$ Hz, 6H, PCH_2), 1.98 (m, 6H, PCH_2), 1.06–1.14 (overlapping multiplets, 27H, PCH_2CH_3). ^{31}P NMR (C_6D_6): δ -12.6 (d, $J = 15.5$ Hz), -17.6 (t, $J = 15.5$ Hz). MS (EI): 593, 595, 597, 599 ($\text{M}^+ - \text{Et}_3\text{P}$), 475, 477, 479, 481 ($\text{M}^+ - 2\text{Et}_3\text{P}$), 118 (Et_3P^+).

Acknowledgment. This work was supported by the Department of Energy.

Supporting Information Available: Full crystallographic details (.cif file) and alcoholysis reactions. This material is available free of charge via the Internet at <http://pubs.acs.org>.

IC020424P